Journal of Applied Spectroscopy, Vol. 69, No. 2, 2002

FOUR-WAVE MIXING IN A NONLINEAR FABRY–PEROT INTERFEROMETER

O. G. Romanov,[a] A. S. Rubanov,[b] and A. L. Tolstik[a*]

UDC 621.372.413

A theoretical model of four-wave mixing in a Fabry–Perot interferometer with resonant nonlinearity has been developed. The conditions for the realization of the effect of interferometer transmission symmetry breaking and the specific features of the formation of space-time structures of light fields have been analyzed. The laws of hysteresis of the lateral laser beam profiles have been established.

Keywords: *four-wave mixing, resonant instability, lateral laser beam profile, Fabry–Perot interferometer.*

The steady interest in nonlinear systems of optical data processing that has been shown in the last few decades is due to the prospects of direct optical image transformation and control of the space-time structure of light fields. The first investigations in this field dating back to the 1960s were developed by generalizing the ideas and methods of traditional (static) holography as applied to the processes of recording and processing the wave fields in nonlinear media. Subsequently, a close relationship between dynamic holography and nonlinear optics was established. The works along these lines revealed the phenomenon of wave-front reversal (phase conjugation) of light beams under four-wave mixing (FWM) [1]. The upsurge of investigations on the phase-conjugation optics in the 1980s set new ways in using dynamic gratings for solving various problems of transformation of the space-time structure of light fields (phase-distortion compensation, radiation self-focusing on a target, associative holographic memory, dynamic grating lasers, etc.) [2].

At the same time, the discovery in the mid-1970s of the phenomenon of optical bistability revealed at light-beam propagation in a nonlinear Fabry–Perot interferometer filled with sodium vapors is noteworthy [3]. The investigations along these lines made it possible to devise a transphasor (an optical analog for the transistor) and optical limiters and to develop an optical memory system. The nonlinear interferometers proved to be very convenient systems for modeling various effects of self-organization. On their basis various dynamic regimes, including regenerative intensity pulsations and the transition to optical chaos were investigated [4]. In the last decade, nonlinear systems for controlling the spatial structure of laser beams received a large development effort [5]. Methods for generating light fields of new types — stationary spatially modulated, rotating, helical, and turbulent — ones were proposed.

Analysis of the interaction of two light waves of equal input intensity at their counterpropagation in a nonlinear ring cavity revealed a new regime of optical bistability in which energy transfer from the less intense light beam to the more powerful one takes place and the effect of interferometer transmission asymmetry for two light beams with a practically equal input intensity is observed [6]. This effect, named asymmetric optical bistability, was also predicted later for the case of symmetric incidence of two light beams on the input mirror of a Kerr-nonlinearity Fabry–Perot interferometer [7]. The dynamics of nonlinear-optical systems under the conditions of symmetry breaking bifurcation was investigated by an example of anisotropic lasers with a saturating absorber [8] as well as in a distributed feedback system (Bragg grating) at counterpropagation of two light beams [9].

[*]To whom correspondence should be addressed.

[a]Belarusian State University, 4 F. Skorina Ave., Minsk, 220050, Belarus; e-mail: tolstik@bsu.by; [b]B. I. Stepanov Institute of Physics, National Academy of Sciences of Belarus, Minsk. Translated from Zhurnal Prikladnoi Spektroskopii, Vol. 69, No. 2, pp. 248–257, March–April, 2002. Original article submitted December 26, 2001.

 0021-9037/01/6902-0286$27.00

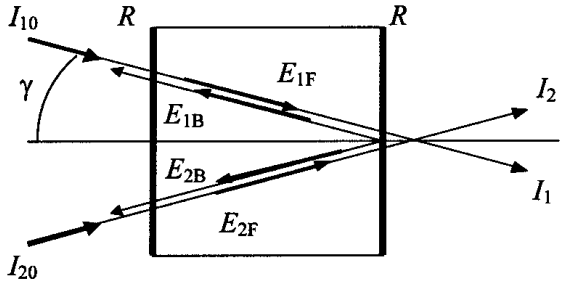

Fig. 1. Scheme of interaction of the light beams in the Fabry–Perot interferometer.

In the present paper, by the methods of theoretical modeling and numerical simulation the laws of the formation of space-time structures of light beams under the conditions of intracavity FWM realized at oblique incidence of two waves on the input mirror of a nonlinear Fabry–Perot interferometer symmetrically about the normal have been investigated. The features of FWM under the conditions of mixed absorption-dispersion bistability with regard for the transient processes, in which the field reaches the steady state in the cavity, and the diffraction mechanism of transverse interaction of the light beams have been analyzed.

Theoretical Model of Four-Wave Mixing in a Nonlinear Fabry–Perot Interferometer. The scheme of FWM in a nonlinear Fabry–Perot interferometer is given in Fig. 1. Two light beams I_{10} and I_{20} are directed into the cavity at a small angle γ with each other symmetrically about the normal to the input mirror surface. When reflected from the output mirror of the interferometer, the waves E_{1F} and E_{2F} create for each other counterpropagating waves E_{1B} and E_{2B} so that inside the cavity degenerate FWM takes place.

The intracavity interaction of the light beams is due to the recording of dynamic gratings in the bulk of the nonlinear layer and the diffraction on them. As a result of the relaxation process in both the nonlinear medium and the cavity, the energy exchange between the waves is nonstationary; therefore, to describe the dynamics of the intracavity FWM, it is necessary to consider the system of reduced wave equations together with the kinetic equations for the components of the Fourier expansion of the medium nonlinear susceptibility in terms of the spatial harmonics of the recorded dynamic grating.

Taking into account the parametric interaction of the light waves and the transverse distribution effects determined by the radiation diffraction, we can write the equations for the slowly varying amplitudes of the light fields in the form

$$\Delta_\perp E_1 + 2ik\left(-\gamma\frac{\partial E_1}{\partial x}+\frac{\partial E_1}{\partial z}+\frac{1}{\nu}\frac{\partial E_1}{\partial t}\right)=-\frac{4\pi\omega^2}{c^2}\left[\chi_0 E_1+\chi_1 E_2\right],$$
$$\Delta_\perp E_2 + 2ik\left(\gamma\frac{\partial E_2}{\partial x}+\frac{\partial E_2}{\partial z}+\frac{1}{\nu}\frac{\partial E_2}{\partial t}\right)=-\frac{4\pi\omega^2}{c^2}\left[\chi_0 E_2+\chi_{-1} E_1\right], \quad (1)$$

where $\Delta_\perp = \frac{\partial^2}{\partial x^2} + \frac{\partial^2}{\partial y^2}$, $v = c/n_0$ is the velocity of light in the medium, and χ_0, χ_1, and χ_{-1} are the expansion components of the medium nonlinear susceptibility $\chi_{nl} = n_0\Delta n/2\pi$ in a spatial Fourier series ($\chi_m = \frac{1}{2\pi}\int_{-\pi}^{\pi}\chi_{nl}\exp[-im(\mathbf{K}\cdot\mathbf{r})]d(\mathbf{K}\cdot\mathbf{r})$; $\mathbf{K} = \mathbf{k}_1 - \mathbf{k}_2$).

We provide a theoretical treatment for a high-Q interferometer in the mean-field approximation, which consists of the procedure of averaging the amplitudes of the interacting fields along the cavity axis and holds in the case of high reflection coefficients of the mirrors ($R \approx 1$), a small optical density of the medium ($kL << 1$), and interferometer tuning close to resonance ($\Phi = 2\pi nL/\lambda \approx m\pi$) [4, 10]. Under such conditions, the amplitudes of the coun-

terpropagating waves can be considered to be equal, $E_{1F} = E_{1B} = E_1$ and $E_{2F} = E_{1B} = E_2$, and the system of coupled wave equations is of the form

$$t_R \frac{\partial E_1}{\partial t} = E_{10} - E_1 + i\Delta_0 E_1 + iC'(\chi_0 E_1 + \chi_1 E_2) + i\beta\Delta_\perp E_1 + \gamma' \frac{\partial E_1}{\partial x},$$
$$t_R \frac{\partial E_2}{\partial t} = E_{20} - E_2 + i\Delta_0 E_2 + iC'(\chi_0 E_2 + \chi_{-1} E_1) + i\beta\Delta_\perp E_2 - \gamma' \frac{\partial E_2}{\partial x}, \quad (2)$$

where $E_{10}(x, y, t)$, $E_{20}(x, y, t)$ is the space-time distribution of the amplitudes of the input light beams at the boundary with the medium ($E_{j0} = \sqrt{8\pi I_{j0}(1-R)/cn_0}$, $j = 1, 2$), $t_R = 2L/v(1 - R)$ is the field settling time in the cavity, $\Delta_0 = 2\Phi_0/(1 - R)$ is the normalized initial detuning of the interferometer from the resonance ($\Phi_0 = 2\pi n_0 L/\lambda - m\pi$), $C' = 4\pi C/n_0\kappa_0$, $C = k_0(\omega)L/2(1 - R)$ is the cooperative parameter ($k_0(\omega)L$ is the optical thickness of the medium), κ_0 is the linear extinction coefficient, $\beta = \lambda L/2\pi(1 - R)$ is the parameter determining the radiation diffraction, and $\gamma' = \gamma L/2n(1 - R)$ is the normalized angle of incidence of the light beams.

We carry out further theoretical analysis in the approximation of a two-level model of the resonant medium, where the nonlinear susceptibility $\chi_{nl} = n_0\Delta n/2\pi$ can be given in the form [11]

$$\chi_{n1} = \frac{n_0\kappa_0}{2\pi}\left(\hat{\Theta}_{12}/B_{12} - \hat{\alpha}I/(1 + \alpha I)\right), \quad (3)$$

where $\hat{\alpha} = a + i\alpha = (\hat{\Theta}_{12} + \hat{\Theta}_{21})/vP_{21}$ is the complex parameter of the two-level resonant medium nonlinearity, whose real part determines the light-induced change in the refractive index and the imaginary part characterizes the change in the absorption coefficient; $\hat{\Theta}_{ij} = \Theta_{ij} + iB_{ij}$, the coefficients $\Theta_{ij}(\omega)$ are related by the Kramers–Kronig (dispersion) relations to the Einstein coefficients $B_{ij}(\omega)$; the parameter $\alpha = (B_{12} + B_{21})/vP_{21}$ determines the resonant transition saturation intensity; P_{21} is the integrated probability of spontaneous and nonradiative transitions.

Using expression (3) and the classical balance equation for the population of the excited energy level, we write the kinetic equation for the nonlinear susceptibility of the medium:

$$\frac{1}{P_{21}}\frac{\partial\chi_{n1}}{\partial t} + \chi_{n1} - \frac{n_0\kappa_0}{2\pi}\frac{\hat{\Theta}_{12}}{B_{12}} = \left(\frac{n_0\kappa_0}{2\pi}\left(\frac{\hat{\Theta}_{12}}{B_{12}} - \frac{\hat{\alpha}}{\alpha}\right) - \chi_{n1}\right)\alpha I. \quad (4)$$

Taking into account the intensity modulation in the bulk of the nonlinear layer under intracavity FWM ($I = \frac{cn_0}{8\pi}(|E_1|^2 + |E_2|^2 + E_1E_2^* \exp(i\mathbf{K}\cdot\mathbf{r}) + E_1^*E_2 \exp(-i\mathbf{K}\cdot\mathbf{r}))$), Eq. (4) permits us to write the system of differential equations for the components of the medium nonlinear susceptibility expansion into a series in terms of dynamic grating spatial harmonics

$$\frac{1}{P_{21}}\frac{\partial\chi_0}{\partial t} = \frac{n_0\kappa_0}{2\pi}\left(\frac{\hat{\Theta}_{12}}{B_{12}} + \left(\frac{\hat{\Theta}_{12}}{B_{12}} - \frac{\hat{\alpha}}{\alpha}\right)\alpha'\left(|E_1|^2\right) + \left(|E_2|^2\right)\right) - \chi_0\left(1 + \alpha'\left(|E_1|^2 + |E_2|^2\right)\right) - \chi_1\alpha' E_1^* E_2 - \chi_{-1}\alpha' E_1 E_2^*,$$
$$\frac{1}{P_{21}}\frac{\partial\chi_1}{\partial t} = \frac{n_0\kappa_0}{2\pi}\left(\frac{\hat{\Theta}_{12}}{B_{12}} - \frac{\hat{\alpha}}{\alpha}\right)\alpha' E_1 E_2^* - \chi_0\alpha' E_1 E_2^* - \chi_1\left(1 + \alpha'(|E_1|^2 + |E_2|^2)\right) - \chi_2\alpha' E_1 E_2^*,$$
$$\frac{1}{P_{21}}\frac{\partial\chi_{-1}}{\partial t} = \frac{n_0\kappa_0}{2\pi}\left(\frac{\hat{\Theta}_{12}}{B_{12}} - \frac{\hat{\alpha}}{\alpha}\right)\alpha' E_1 E_2^* - \chi_0\alpha' E_1^* E_2 - \chi_{-1}\left(1 + \alpha'(|E_1|^2 + |E_2|^2)\right) - \chi_{-2}\alpha' E_1 E_2^*, \quad (5)$$

. . . . . .

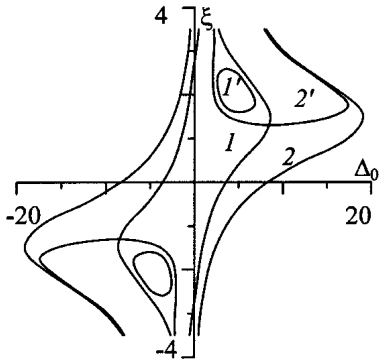

Fig. 2. Domain of existence of symmetric (1, 2) and asymmetric (1′, 2′) optical bistability; $C(\omega_{12}) = 15$ (1, 1′) and 30 (2, 2′).

$$\frac{1}{P_{21}}\frac{\partial \chi_n}{\partial t} = \chi_{n-1}\alpha' E_1 E_2^* - \chi_n\left(1 + \alpha'\left(|E_1|^2 + |E_2|^2\right)\right) - \chi_{n+1}\alpha' E_1^* E_2 ,$$

where $\alpha' = \alpha\dfrac{cn_0}{8\pi}$. Restricting ourselves to the zero and first expansion components, by the first three equations of system (5) together with the system of equations (2) we can describe the process of degenerate FWM in the Fabry–Perot interferometer with resonant nonlinearity at an arbitrary ratio between the intensities of the light beams incident on the interferometer I_{10} and I_{20}. Let us dwell on the case of interaction of beams of equal intensities where the problem becomes symmetrical about the waves E_1 and E_2. In this case, as with the Kerr nonlinearity interferometer [7], one would expect the manifestation of the effect of asymmetric optical bistability.

Optical Bistability and Transmission Asymmetry of the Nonlinear Interferometer. We first carry out the analysis of the asymmetric optical bistability and the conditions for its realization in the plane-wave approximation. The stationary solution of the system of differential equations (2), (5) permits us to write a system of transcendental equations relating the light-beam intensities at the input ($I_{10} = I_{20} = I_0$) and the output (I_1, I_2) of the interferometer:

$$I_0 = I_j\left[\left\{1 + \frac{2C}{A_0}(1 + \tilde{\alpha} I_j)\right\}^2 + \left\{\Delta_0 + \frac{a}{\alpha}\frac{2C}{A_0}(1 + \tilde{\alpha} I_j)\right\}^2\right], \tag{6}$$

where $j = 1, 2$; $A_0 = 1 + 2\tilde{\alpha}(I_1 + I_2) + \tilde{\alpha}^2(I_1^2 + I_2^2)$; $\tilde{\alpha} = \alpha(1 - R)$, the coefficient $(1 - R)$ determines the difference between the intensities at the interferometer output and inside the resonant medium. Hereinafter we consider a two-level model with coinciding absorption and emission profiles, for which $\hat{\Theta}_{12}/B_{12} = \hat{\alpha}/\alpha$.

The symmetrical solution of the system of equations (6) corresponds to equal intensities of the light beams at the interferometer output ($I_1 = I_2 = I$). In this case, system (6) transforms to one equation:

$$I_0 = I\left[\left\{1 + \frac{2C}{A_0}(1 + \tilde{\alpha} I)\right\}^2 + \left\{\Delta_0 + \frac{a}{\alpha}\frac{2C}{A_0}(1 + \tilde{\alpha} I)\right\}^2\right], \tag{7}$$

where $A_0 = 1 + 4\tilde{\alpha} I + 2\tilde{\alpha}^2 I^2$.

Analysis of Eq. (7) shows that the transmission function of the interferometer under certain conditions (cooperative parameter C values, radiation frequency detuning from the absorption band center (determining the ratio a/α), and detuning from the interferometer resonance Δ_0) can be characterized by an S-shaped bistable loop. The domain of existence of optical bistability on the plane of parameters — interferometer detuning from resonance Δ_0, radiation frequency detuning from the absorption profile center ξ — is given in Fig. 2 (curves 1, 2). Calculations have been performed for the Gaussian approximation of coinciding absorption and emission profiles.

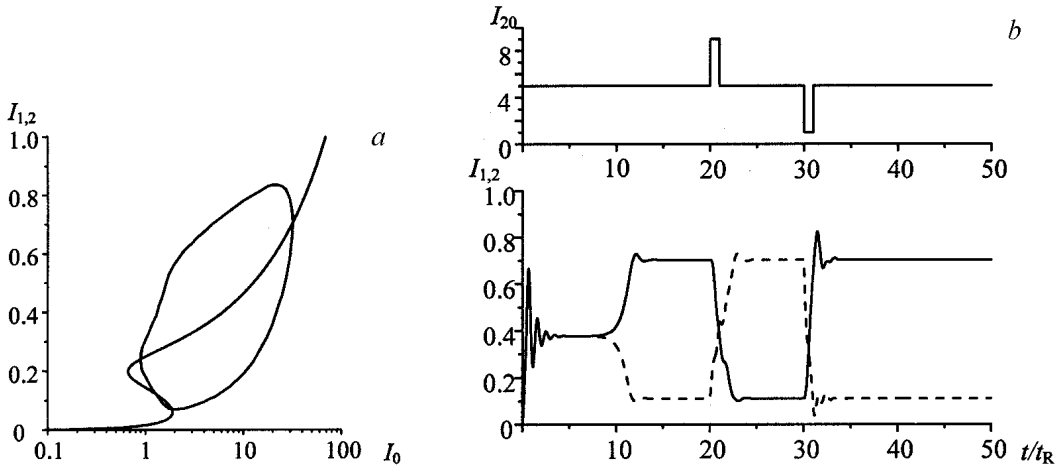

Fig. 3. Stationary transmission function of the interferometer (a) for two light beams in the domain of existence of asymmetric optical bistability ($C(\omega_{12})$ = 35, Δ_0 = –15, ξ = –2) and dynamics of interferometer switching (b) between different transmission levels for two light waves (I_1, solid line, I_2, dashed line) at a short-term change in the wave intensity I_{20}. The master pulse amplitude ΔI = 4 (the wave intensities are normalized to the saturation intensity of the resonant transition $I_{sat} = \alpha^{-1}$).

At the same time, under certain conditions, an asymmetric solution of the system of equations (6) characterized by inequality of emergent beam intensities $I_1 \neq I_2$ is possible. The typical dependence of intensities at the interferometer output I_1, I_2 on the input intensity (I_{10}, $I_{20} = I_0$) is given in Fig. 3a. It is seen that in a certain range of input intensity I_0 values, along with the symmetric solution (the upper branch of the *S*-shaped curve), there exists a new solution where intensities I_1 and I_2 can assume values one of which corresponds to the upper and the second to the lower part of the circular region. It should be noted that from the point of view of the stationary model, as follows from the symmetry of the problem, one cannot guess which of the intensities (I_1 or I_2) will be larger.

The procedure of finding the asymmetric regime of optical bistability consists of solving the system of transcendental equations (6) with the use of the values of the light wave intensities I_1 and I_2 as independent variables. The domain of parameters at which asymmetric optical bistability is realized is given in Fig. 2 (curves 1′ and 2′). It is seen that the asymmetric solution appears against the background of classical optical bistability.

The standard procedure of linear analysis of the stability of the steady-state regimes of intracavity FWM makes it possible to classify the bifurcations characteristic of the system of coupled wave equation (2). As shown in [12], for the Kerr model of intracavity material nonlinearity the regime of optical bistability is realized due to the saddle-node bifurcation and the asymmetric regime of interaction results from the pitchfork bifurcation of the symmetric solution. According to the classification of local bifurcations [13], pitchfork bifurcations are characteristic of nonlinear systems exhibiting the property of mirror symmetry. The problem under consideration is symmetric about the normal to the input mirror of the interferometer (change of indices $1 \leftrightarrow 2$ in Eqs. (2)) and, therefore, has prerequisites for the manifestation of the symmetry-breaking bifurcation. The physical meaning of this phenomenon becomes clear when the notion of potential energy of the system is used: a potential with one minimum corresponding to the symmetric solution (stable equilibrium state) transforms into a potential with two minima corresponding to two stable asymmetric solutions and an intermediate maximum corresponding to the unstable symmetric solution.

Let us analyze the conditions for the realization of asymmetric regimes of FWM. As seen from Fig. 2, the domain of existence of asymmetric optical bistability is in the 1st and 3rd quadrants of the plane (Δ_0, ξ), which complies with the requirement on coincidence of the signs of the initial detuning of the cavity from the transmission peak and of the radiation frequency detuning determining the sign of the nonlinear change in the refractive index. In so doing, the laser radiation frequency detuning from the absorption band center should exceed a certain value depending

on the cooperative parameter $C(\omega_{12})$. With increasing cooperative parameter the critical value of the frequency detuning decreases, tending to one halfwidth of the Gauss profile of absorption.

Note the impossibility of realizing asymmetric optical bistability both at the center of the medium absorption band ($\xi = 0$) and for tuning the interferometer to the transmission maximum ($\Delta_0 - 0$). The first fact is a consequence of recording pure amplitude dynamic gratings that are due to the modulation of the absorption coefficient ($a/\alpha = 0$). As follows from the equations for the complex amplitudes (2), in this case the phase difference between the light waves does not vary with time. The inclusion of phase gratings increases the energy-exchange efficiency and when the critical interaction length (determined by the cooperative parameter C) is exceeded it leads to the symmetry-breaking bifurcation. Numerical analysis has shown that the asymmetric regime of bistability takes place at $C > C_{cr}(\omega_{12}) \approx 12$. Note that for optical bistability $C_{thresh} = 4$ [4].

To determine the initial interferometer detuning from resonance $\Delta_0 = 2\Phi_0/(1 - R)$ needed for the realization of asymmetric optical bistability, we consider the dependence of the light-induced phase detuning of the interferometer $\Phi = 2\pi nL/\lambda - m\pi$ on the spectroscopic parameters of the resonant medium. Taking into account the formula for the nonlinear susceptibility (3), we can write the expression for the detuning in the form

$$\Phi = \Phi_0 + \frac{k_0 L}{2}\left(\frac{\Theta_{12}}{B_{12}} - \frac{\alpha I}{1+\alpha I}\right).$$

For the resonant medium with coinciding profiles of absorption and emission ($\Theta_{12}/B_{12} = a/\alpha$) the expression for the phase detuning transforms to the form

$$\Phi = \Phi_0 + \frac{k_0 L}{2}\frac{a}{\alpha}\frac{1}{1+\alpha I}.$$

From this it follows that for working in the region of the interferometer transmission maximum ($\Phi \approx 0$), the initial detuning Φ_0 and the factor $a/\alpha = \Delta n/\Delta\kappa$ should have opposite signs. Since $\Delta\kappa < 0$ for all values of the radiation frequency detuning from the absorption-band center (bleaching effect), the above condition is met for $\Phi_0 > 0$ in the short-wave region of the spectrum ($\Delta n > 0$, $\xi > 0$, 1st quadrant of the plane (Δ_0, ξ) in Fig. 2) and for $\Phi_0 < 0$ in the long-wave region ($\Delta n < 0$, $\xi < 0$, 3rd quadrant of the plane (Δ_0, ξ)). At the initial tuning of the interferometer to the transmission maximum ($\Phi_0 \approx 0$) a light-induced change in the refractive index leads to its detuning from the transmission peak, a decrease in the radiation intensity in the medium, and a decrease in the efficiency of energy exchange between the light beams, preventing the realization of the regime of asymmetric optical bistability.

Thus, the reason for the appearance of asymmetric solutions of the system of differential equations (2) describing the FWM process in the nonlinear cavity is the account of the processes of parametric energy exchange between the light waves and its essentially nonlinear character. In media with resonant nonlinearity, the leading role in the energy exchange leading to the interferometer transmission symmetry breaking is played by the refractive index gratings (phase gratings) determining the phase mismatch of the interacting waves. Comparing the obtained conditions for the realization of asymmetric optical bistability under FWM in the interferometer with the conditions for observing bistability in the noncavity regime of FWM in resonant media [12], it can be noted that in the interferometer realizing an additional kind of feedback on reflection from the cavity mirrors, the threshold values of the optical density of the nonlinear layer and the incident radiation intensity decrease considerably due to the multiple rereflection of the radiation. Another feature of FWM in the nonlinear interferometer is a decrease in the threshold values of laser radiation frequency detuning from the absorption profile center. For instance, for the realization of optical bistability in a noncavity scheme of FWM it is necessary that the laser radiation frequency be detuned by 1.4 profile half-widths [14], whereas for the interferometer the detuning by one half-width is enough. Note that the recalculation of the above threshold values for the case of the Lorentzian spectral shape of the profile yields 3.5 profile half-widths for the noncavity scheme of FWM and 1.5 half-widths for the FWM in the interferometer.

Transient Processes and Dynamics of Intracavity FWM under Asymmetric Optical Bistability. Analysis of the transient processes under FWM in the interferometer is first carried out in the approximation of instantaneous nonlinearity ($t_R P_{21} >> 1$) where the response of the medium to the acting radiation is formed much faster than the field in the cavity reaches its steady state. Such a situation can be realized for both fast-relaxing media and high-Q

interferometers. The above approximation allows us, in describing the intracavity FWM, to disregard the kinetic equations (5) and restrict ourselves to the system of equations (2) with the replacement of the nonlinear susceptibility components χ_0 and $\chi_{\pm 1}$ by their stationary values:

$$\chi_0 = \frac{n_0 \kappa_0}{2\pi}\left(\hat{\Theta}_{12}/B_{12} - \hat{\alpha}/\alpha + \hat{\alpha}/\alpha A_0\right),$$

$$\chi_1 = -\frac{n_0 \kappa_0 \hat{\alpha}' E_1 E_2^*}{\pi A_0 (1 + \alpha'(|E_1|^2 + |E_2|^2) + A_0)}, \tag{8}$$

$$\chi_{-1} = -\frac{n_0 \kappa_0 \hat{\alpha}' E_1^* E_2}{\pi A_0 (1 + \alpha'(|E_1|^2 + |E_2|^2) + A_0)},$$

where $A_0 = (1 + 2\alpha'(|E_1|^2 + |E_2|^2) + \alpha'^2(|E_1|^2 - |E_2|^2)^2)^{1/2}$.

Figure 3b gives an example of the characteristic dependence of the radiation intensity at the interferometer output on time under the conditions of symmetry-breaking bifurcation. It is seen that in time $t \approx 3t_R$ after several oscillations about the transmission peak the field inside the cavity reaches the quasi-steady state corresponding to the symmetric solution of the system of equations (2). Then, because of the instability of this solution, the system goes to states with a different level of transmission. Note that the speed of progress of this process is proportional to the intensity difference of the interacting waves at the interferometer input (in numerical simulation, we chose the deviation $\Delta I/I_0 \sim 10^{-7}$). The instability of the symmetric solution makes it possible to easily realize the regime of optical switchings (Fig. 3b). Once a stable state with a high level of transmission for one beam (I_1) and a low level for the other (I_2) has been reached, we can switch the transmission levels by feeding a positive pulse to the less intense beam ($t = 20t_R$) or a negative pulse to the more intense beam ($t = 30t_R$). In either case, after relaxation oscillations the interferometer is switched to the state opposite to the initial one. The amplitude and duration of the switching signal should be strong enough to pass through the unstable state of equal transmission of both beams. Then the process of directional energy exchange develops and the interferometer goes to a state with a considerably different level of transmission for the two beams.

More complex dynamic modes of operation of the interferometer can be obtained by taking into account the sluggishness of the light-induced response described by the system of kinetic equations (5). The typical dynamic modes of operation under the conditions where the relaxation time of the medium is larger than the settling time of the field in the cavity ($t_R P_{21} = 0.1$) are given in Fig. 4. The interferometer parameters were chosen the same as for the stationary case (Fig. 3a). At the input radiation intensity $\alpha I_0 = 2$ slightly exceeding the intensity at which the interferometer is switched to the state with a high transmission, the interferometer first goes slowly (in time $\sim 150t_R$) to the state with equally high transmission for the two beams. Then, as in the case of instantaneous nonlinearity, the symmetric state breaks down due to the symmetry-breaking bifurcation. The break-down rate of the symmetric state depends on the input intensity difference of the light waves (it was chosen between 10^{-7} and 10^{-4}). However, this parameter produced no significant influence on the character of subsequently realized oscillations. As seen from Fig. 4a, the stationary asymmetric solution of the system of coupled wave equations at the chosen parameters proves to be unstable towards the bifurcation of the limit cycle generation, and the output intensities of the two beams are characterized by regular pulsations. Since self-oscillations occur in the vicinity of asymmetric stationary values of intensities of the two beams and have opposite phases, such a regime is called asymmetric self-pulsations. With increasing input intensity the amplitude and frequency of oscillations change, in which case the amplitude increases and the frequency monotonically decreases (Fig. 4a–4c). Figure 5a shows the phase "portrait" of this type of oscillations on the plane of parameters (I_1, I_2) representing a localized closed trajectory. The dynamics of the two light waves is characterized by a change in the intensity from the symmetric state to the state with a high transmission for one wave and a low transmission for the second wave.

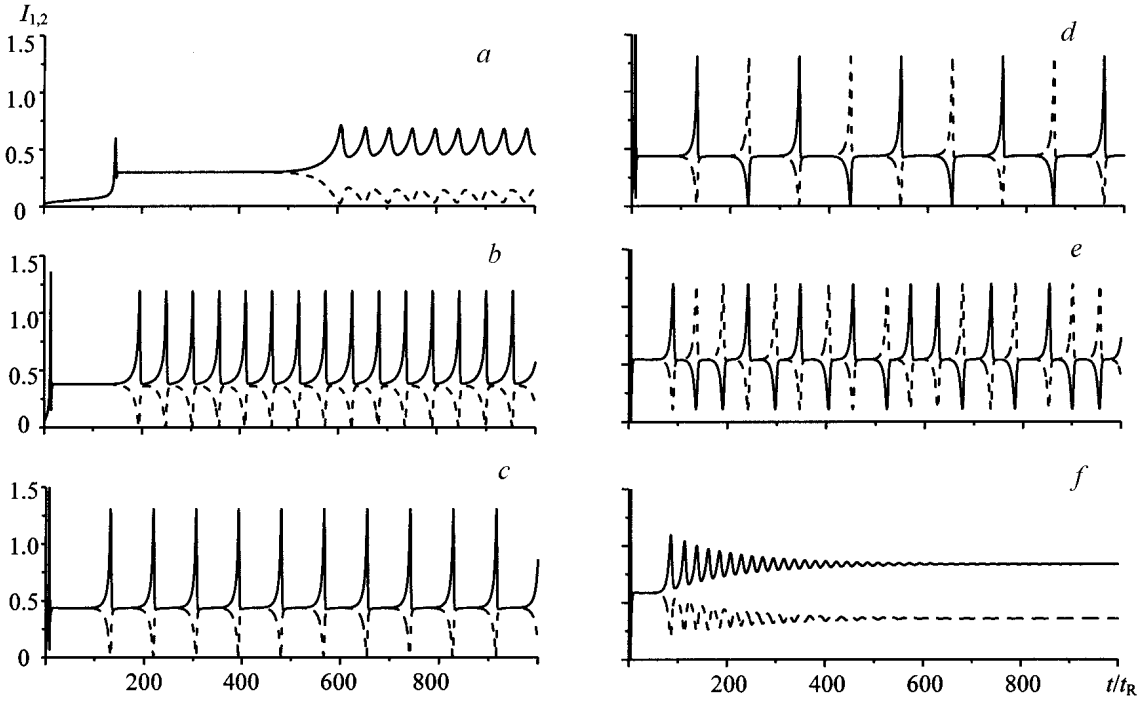

Fig. 4. Transmission dynamics of the interferometer at the input intensity of the light waves αI_0 = 2 (a), 5 (b), 8.22 (c), 8.23 (d), 16 (e), and 20 (f); a, b, c) asymmetric; d) switched; e) chaotic; f) decaying self-pulsations.

Further increase in the input intensity leads to the switching of the system to a new dynamic state (Fig. 4d). The intensity of the light waves varies between three unstable states — one symmetric and two asymmetric states. It should be noted that now both waves can reach the states with a high and a low level of transmission. The shape of the time dependences of intensities of both waves permit calling such a regime switching oscillations. In this case, the phase "portrait" changes as well (Fig. 5b). The process reverse to the symmetry-breaking bifurcation at which the asymmetric mechanical trajectory on the plane of parameters (I_1, I_2) transforms to a symmetric one proceeds. The transition from asymmetric to switching oscillations is accompanied by significant changes in the corresponding Fourier spectra as well (Fig. 5d, 5e). The only frequency characteristic of the regime of asymmetric oscillations breaks down into two. One of them (f_1) corresponds to the process of reproduction of the general form of oscillations, i.e., it determines the time of switching from the symmetric to the asymmetric solution regardless of the particular number of the wave being switched. The second frequency (f_0) is equal in magnitude to half of the first one and determines the switching between different levels of transmission for each wave. Since the frequencies f_0 and f_1 are related by the relation $f_1 = 2f_0$, it can be stated that the Fourier spectrum (Fig. 5e) consists of even $(f_1)_n = 2nf_0$ (n = 1, ∞) and uneven $(f_0)_n = 2(n - 1)f_0$ harmonics of f_0 oscillations, with the uneven harmonics being more prominent.

With further increase in the input intensity the interaction dynamics of the two beams becomes chaotic. In this case, the intensity oscillations of the two light beams between three different states are irregular (Fig. 4e) and the Fourier spectrum does not have any marked frequencies (Fig. 5f). With the chosen parameters this regime is realized in the range of input intensity values αI_0 = 15.9–16.1. At the boundaries of the domain of realization of asymmetric optical bistability we have the reverse transition from irregular self-pulsations to the regime of stable solutions through dying oscillations (αI_0 = 20, Fig. 4f).

Thus, when the input intensity is changed, in the domain of existence of asymmetric optical bistability a sequence of various self-oscillation regimes is observed: asymmetric self-pulsations (Fig. 4a–4c) — switching self-pulsations (Fig. 4d) — irregular self-pulsations (Fig. 4e) – asymmetric self-pulsations (similar to Fig. 4a–4c) — stable asymmetric equilibrium states (Fig. 4f). The presence in the nonlinear dynamic system under consideration of a bifurcation of limit cycle generation and a pitchfork bifurcation makes it possible to modulate, in a complicated manner,

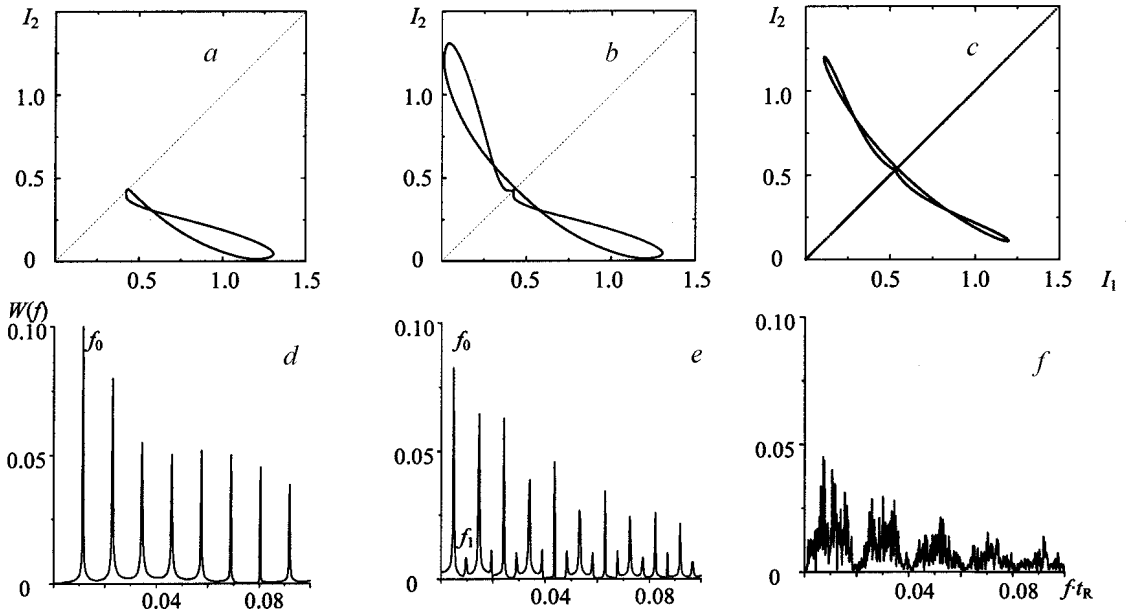

Fig. 5. Phase portraits (a–c) and their corresponding Fourier spectra (d–f) for various self-oscillations of the light-beam intensities at the interferometer output; αI_0 = 8.22 (a, d), 8.23 (b, e), and 16 (c, f).

the radiation passed through the interferometer, with the frequency and amplitude of realized oscillations depending on both the input intensity and the nonlinear interferometer parameters.

Transverse Structure of Light Beams under FWM in the Nonlinear Interferometer. Let us discuss the influence of the transverse distribution effects caused by the radiation diffraction on the formation of transverse profiles of light-beam intensities under the conditions for realization of optical bistability in a nonlinear interferometer. As is known [5], for distributed optical systems exhibiting the property of bistability the presence of even a weak transverse interaction is of fundamental importance. In its absence, a wide incident collimated beam can be split into individual noninteracting longitudinal ray tubes and we can make use of the transfer function of the point system for each individual tube. With such a procedure, in the case where the maximum intensity of the input signal is higher than the switching intensity of the system to a state with a high transmission, a nonphysical profile of the output radiation intensity will be obtained. This is due to the fact that for a distributed system the condition for spatial switching between the lower and upper branches of the transfer function is not known in advance, and this condition does not coincide with the criterion for temporal switching of the point system. In a distributed system, the account of an even weak transverse interaction of ray tubes leads to the formation of a switching wave between the states corresponding to different branches of the transfer function and the formation of a profile with sharp space boundaries.

The problem of FWM in the nonlinear interferometer was solved by constructing a differential-difference approximation of the system of coupled wave equations (2) according to the two-layer explicit scheme first in the instantaneous nonlinearity approximation. Numerical simulation was performed for the Gaussian light beams and the defocusing type of resonant medium nonlinearity (radiation detuning from the absorption-profile center to the long-wavelength region of the spectrum). The medium and radiation parameters satisfied the condition for the realization of asymmetric optical bistability in the plane-wave approximation. The characteristic spatial intensity distributions of the two light beams at the interferometer output are shown in Fig. 6. As is seen, at the initial stage of the light-field formation in the interferometer the central part of the light beams is switched (Fig. 6a). Then, as a result of the oblique incidence of the light beams on the interferometer, the transverse drift leads to an efficient energy transfer and symmetry breaking in each local part of the light beam. The initially equal profiles of the light beams (Fig. 6a, 6b) corresponding to the symmetric solution of the system of equations (2) are transformed to mirror symmetric profiles (Fig. 6d–6f) with a sharp switching front between the parts of the profile with high and low values of intensity. The inten-

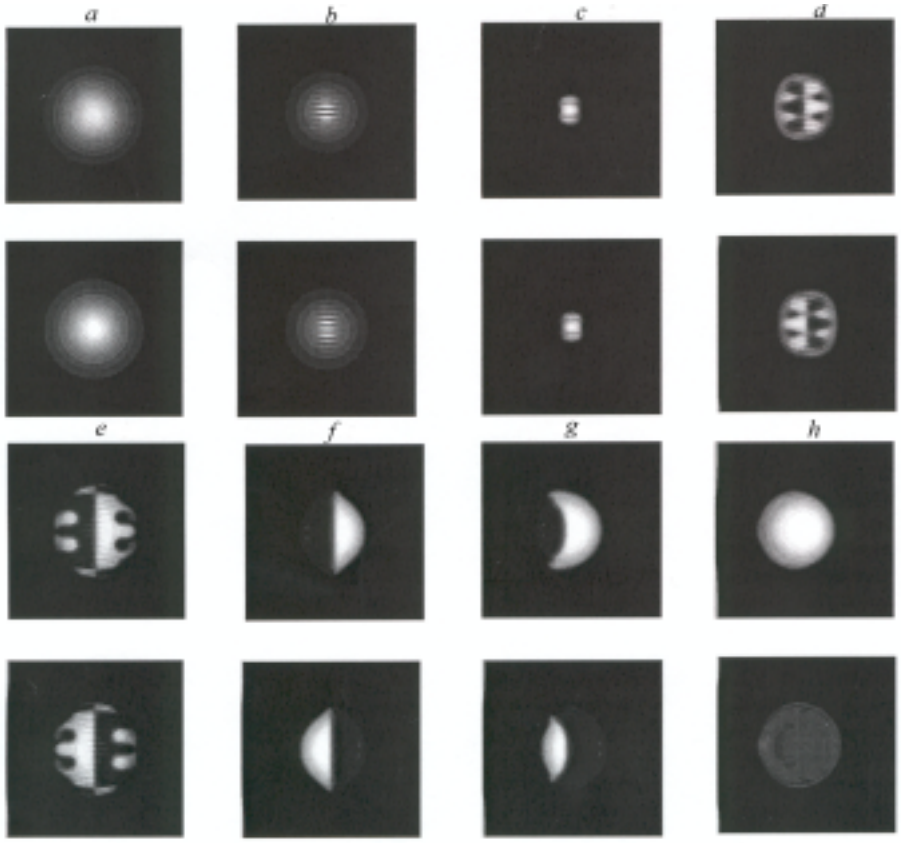

Fig. 6. Intensity distribution in the cross section of the light beams I_1 (upper row) and I_2 (lower row) at instants of time $t = 5t_R$ (a), $10t_R$ (b), $12.5t_R$ (c), $15t_R$ (d), $17.5t_R$ (e), $62.5t_R$ (f), $150t_R$ (g), $250t_R$ (h). At $t = 100t_R$, the intensity of the first light beam I_{10} has been increased in a pulsed manner; $\beta/x_0^2 = 10^{-2}$, $\gamma = 10^{-2}$.

sities of both beams thereby remain equal, and the effect of transmission symmetry breaking appears as profile asymmetry. In each beam the energy is redistributed over the cross section so that the more intense part of the beam remains in the half-plane from which its incidence on the interferometer occurs. This steady state can be switched to a state with a considerably different intensity level for the two beams by increasing or decreasing in a pulsed manner the input intensity of one of the beams (Fig. 6g, 6h). In this case, as in the plane-wave approximation, along with the spatial hysteresis of the intensity distribution in the cross section of the light beams the total intensity hysteresis is realized.

Note that the realization of both possible variants of the transverse intensity distribution of the light beams at the interferometer output is determined by the competition between two processes — the transverse drift of the radiation in the interferometer due to the oblique incidence of the light beams and the energy exchange between the beams on the dynamic gratings being recorded [15]. At small angles of incidence an integral process of directional energy exchange develops and the light-beam intensities at the interferometer output can differ significantly. In this case, the time dependences of the integrated intensity of the light beams remain the same as for the transmission symmetry-breaking bifurcation in the plane-wave approximation (Fig. 3b, at $t/T_R < 20$). With increasing angle of incidence, the transverse shift of the light beams at multiple rereflection from the interferometer mirrors decreases the efficient interaction time, at which energy exchange between the beams occurs, and leads to the formation of beams with a mirror symmetric spatial distribution of intensity. At large values of the angle of incidence, the light beams pass through each other practically without experiencing energy exchange and remain equal, retaining their initial Gaussian form.

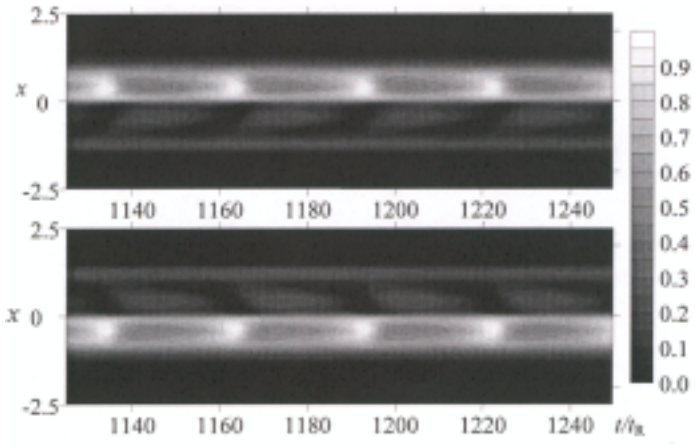

Fig. 7. Dynamics of the intensity distribution in the transverse profile of the light beams under the conditions for realization of asymmetric self-pulsations; $t_R P_{21} = 0.1$, $C(\omega_{12}) = 35$, $\alpha I_0 = 5$, $\beta/x_0^2 = 10^{-2}$, $\gamma = 10^{-2}$.

More complex space-time structures can be observed when the response time of the medium is comparable to the settling time of the field in the cavity. Figure 7 shows the results of the numerical simulation at an angle of incidence corresponding to the condition for the formation of mirror-symmetric intensity profiles. The transverse coordinate x is normalized to the half-width of the Gaussian profile of intensity x_0 at the interferometer output. The above-considered property of phase opposition of asymmetric oscillations (Fig. 4) is manifest here as well, but it is only exhibited by individual portions of each light beam.

Conclusions. On the basis of the theoretical analysis of the developed model of FWM in a Fabry–Perot interferometer with resonant nonlinearity, it is shown that along with the regime of optical bistability under FWM in a nonlinear interferometer, the realization of asymmetric optical bistability is possible. Symmetry breaking of the interferometer transmission is due to the pitchfork bifurcation of the symmetric solution. The cause of the appearance of transmission asymmetry is the distributed feedback in the bulk of the nonlinear medium resulting from the diffraction by the phase dynamic gratings. The nonstationary energy exchange between the light beams determines the possibility of realizing various regimes of regular and chaotic self-pulsations of the output radiation intensity at a constant intensity at the interferometer input. On the basis of the analysis of the spatial aspects of the interaction between the light beams, conditions for the realization of a hysteresis of the spatial profiles of the beams and ways of forming complex space-time structures of radiation have been determined.

REFERENCES

1. B. I. Stepanov, E. V. Ivakin, and A. S. Rubanov, *Dokl. Akad. Nauk SSSR*, **196**, 567–571 (1971).
2. A. S. Rubanov (ed.), *Reversal of a Wave Front of Laser Radiation in Nonlinear Media* [in Russian], Coll. of Sci. Papers, Minsk (1990).
3. H. M. Gibbs, S. L. McCall, and T. N. C. Ventkatesan, *Phys. Rev. Lett*., **36**, 1135–1138 (1976).
4. H. M. Gibbs, *Optical Bistability. Light Control by Light* [Russian translation], Moscow (1988).
5. N. N. Rozanov, *Optical Bistability and Hysteresis in Distributed Nonlinear Systems* [in Russian], Moscow (1997).
6. A. E. Kaplan and P. Meystre, *Opt. Commun*., **40**, 229–232 (1982).
7. M. Haelterman, P. Mandel, J. Danckaert, H. Thienpont, and I. Veretennicoff, *Opt. Commun.*, **74**, 238–244 (1989).
8. S. V. Sergeyev and G. G. Krylov, *Opt. Commun*., **139**, 270–286 (1997).
9. Yu. A. Logvin and V. M. Volkov, *JOSA (B)*, **16**, 774–780 (1999).
10. L. A. Lugiato and C. Oldano, *Phys. Rev*., **37**, 3896–3908 (1988).

11. V. V. Kabanov and A. S. Rubanov, *Dokl. Akad. Nauk BSSR*, **24**, 34–37 (1980).
12. I. N. Agishev, E. A. Mel'nikova, O. G. Romanov, and A. L. Tolstik, *Vestn. Bel. Gos. Univ., Ser. 1*, No. 1, 15–19 (2001).
13. V. S. Anishchenko, *Complex Oscillations in Simple Systems* [in Russian], Moscow (1990).
14. V. V. Kabanov, A. S. Rubanov, A. L. Tolstik, and A. V. Chaley, *Opt. Commun.*, **71**, 219–223 (1989).
15. O. G. Romanov, A. S. Rubanov, and A. L. Tolstik, *Litovsk. Fiz. Zh.*, **39**, 250–256 (1999).